POLITECNICO DI TORINO
Repository ISTITUZIONALE

Road to virtual tuning: New physical lump model and test protocol to support damper tuning in hyundai motor Europe technical center

Original
Road to virtual tuning: New physical lump model and test protocol to support damper tuning in hyundai motor Europe technical center / Salgarello, Alessandro; Pizzuto, Antonino; Hahn, Daniel; Ferraris, Alessandro; Airale, Andrea Giancarlo; Carello, Massimiliana. - In: SAE TECHNICAL PAPER. - ISSN 0148-7191. - ELETTRONICO. - 2019:(2019). (Intervento presentato al convegno SAE World Congress Experience, WCX 2019 tenutosi a Cobo Center, usa nel 2019) [10.4271/2019-01-0855].

Availability:
This version is available at: 11583/2731936 since: 2019-05-03T12:18:30Z

Publisher:
SAE International

Published
DOI:10.4271/2019-01-0855

Terms of use:

This article is made available under terms and conditions as specified in the corresponding bibliographic description in the repository

Publisher copyright

(Article begins on next page)

25 April 2024

Road to virtual tuning: new physical lump model & test protocol to support damper tuning in Hyundai Motor Europe Technical Center

A.Salgarello, A. Pizzuto**, Daniel Hahn**, A. Ferraris*, A.G.Airale*, M. Carello*,**
*Politecnico di Torino – Mechanical and Aerospace Engineering Department- Turin - Italy
** Hyundai Motor Europe Technical Center GmbH - Germany

Abstract

Vehicle dynamics is a fundamental part of vehicle performance.
It combines functional requirements (i.e. road safety) with emotional content ("fun to drive", "comfort"): this balance is what characterizes the car manufacturer (OEM) driving DNA.
To reach the customer requirements on Ride & Handling, integration of CAE and testing is mandatory. Beside of cutting costs and time, simulation helps to break down vehicle requirements to component level.
On chassis, the damper is the most important component, contributing to define the character of the vehicle, and it is defined late, during tuning, mainly by experienced drivers. Usually 1D lookup tables Force vs. Velocity, generated from tests like the standard VDA, are not able to describe the full behavior of the damper: different dampers display the same Force vs. Velocity curve but they can give different feeling to the driver. Consequently, the capability to represent the full damper behavior, in testing and numerical simulation, is fundamental.
To do that, a new CAE damper model and an advanced testing protocol have been developed in collaboration between Hyundai Motor Group and Politecnico di Torino. The model has been developed in Matlab/Simulink® to be integrated with the CAE process used in HMETC (e.g. Driving Simulator).
It represents the damper behavior by the physics of its components (such as rod, valves components, etc.). Most of the parameters are sourced from damper BIM or by measuring them. The model has been verified against the output of the testing protocol, showing a good level of correlation up to 30 Hz.
The test protocol has been developed to provide more detailed informations about the damper force evolution under quasi-static and dynamic conditions.
A new way to analyze results in frequency domain has been proposed, to better understand, describe and correlate the damper performance to whole vehicle behavior.

Introduction

Vehicle dynamics is a fundamental part of vehicle performance, for traditional (with internal combustion engine) or hybrid vehicles (range extended, parallel or series, fuel cell) [1, 10].
The shock absorber is an important component in the vehicle chassis, dissipating the energy of a shock by transforming it into heat, due to friction [8, 9, 10]. The excitation can be caused by an irregularity coming from the ground or by the motion of the car body. One of the main purposes of vehicle dynamics study is to define how a shock is transmitted to the passengers, through springs, dampers and anti-roll bars design. The spring is used to absorb the shock, while the damper is used to dissipate the energy of the shock.
Hyundai Motor Group (HMG) has improved a lot the dynamic behavior of their cars in the past few years. One reason of this improvement is the daily effort of the teams working on vehicle dynamics in Hyundai Motor Europe Technical Center (HMETC).
Focusing on improvements, they wanted to have a better knowledge about damper: how the damper is working, how to define its characteristic, how to better judge different shock absorbers (i.e. different suppliers or different tunings) and how to obtain a realistic behavior of the damper in CAE.
The paper shows the development and validation of the damper model and the new testing protocol. The knowledge coming from modeling was used to improve the tests protocol while the results coming from the protocol were used to improve the model itself.
The model developed in HMETC has two main purposes. The first one is to better simulate the behavior of the damper in comparison with the 1D lookup table (Figure 1). Especially at high frequency the hysteresis can not be simulated by the look-up table while it is essential to better correlate the ride behavior of the vehicle.

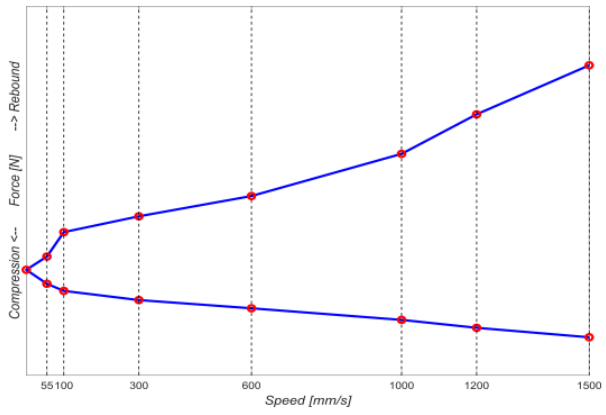

Figure 1. Force vs. Speed– Standard VDA

The second purpose is to use it as a tool in order to be able to virtually tune the damper. Already in the pre-development phase, when the vehicle is still virtual, the damper model can represent the single component properties, giving preliminary indications and a working direction to the tuner.

Advanced Damper Model

S. Duym [11, 12] has developed a model of a damper to be able to simulate the shock absorber behaviour, which can be easily adapted to measurements and is fast to be correlated.
The major weak point, from HMETC perspective, is the modelling of the valve. In its equations, the model is using estimated parameters, instead of ones connected to the properties of the components. The approach to build a model by parts properties, defined by their measurable and distinct values (i.e. the diameter or the thickness of a disc), should lead to a model capable not only to reproduce the behaviour of a given damper, but also to estimate the sensitivity of the damper due to a change in its construction properties.
The advantages of such a model, for an automotive OEM company (like Hyundai), are the possibility to tune the damper on a virtual level as well as to understand the (cross-) influences of different properties on the system.
Based on the Duym Model, a lot of effort has been spent to define a valve model, where the main focus was the representation of the component relevant properties.
The developed shock absorber model is referring to a twin-tube rear shock absorber with a full-displaced piston valve and a classic rod-displaced base valve. It has been built in Simulink, defining the parameters in a Matlab script. The parameters are obtained from the technical drawing, the shock absorber BIM or extracted from the physical component.
For correlation and validation of the model, the tests described in the further section have been used, as a consequence, the model has been tested up to 30 Hz.

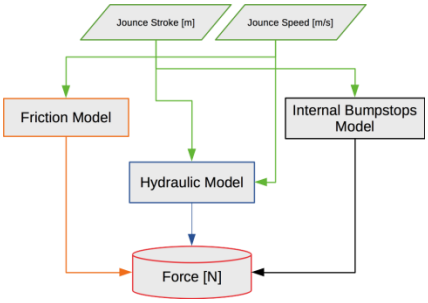

Figure 2. ADM Structure Overview

From now on, the paper will refer to this model as the Advanced Damper Model ADM. The ADM, as shown in figure 2, is composed by three different sub-models that allow to evaluate the three forces components:

1. Hydraulic Model ($F_{hydraulic}$), made by:
    a. Pressure Sub-Model,
    b. Valve Sub-Model.
2. LuGre Friction Model ($F_{friction}$).
3. Internal Bumpstop Model (characteristic Force vs. Displacement curve ($F_{internal\ bumpstops}$).

The sum of the forces evaluated by each model gives the damping force $F_{damping}$ of the simulated shock absorber:

$$F_{damping} = F_{hydraulic} + F_{friction} + F_{internal\ bumpstops} \qquad (1)$$

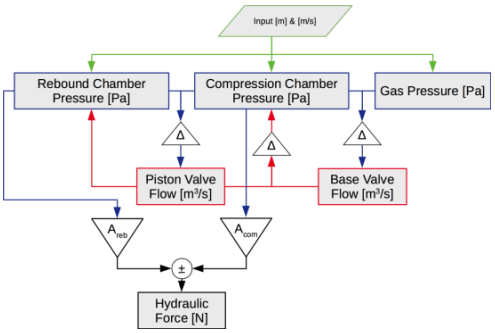

Figure 3. Hydraulic Model Overview

Hydraulic Model

The hydraulic model (Figure 3) is the core of the ADM. It takes as input the amplitude and the speed of the piston rod movement and it delivers as output the force caused by the fluid dynamic effects. The force delivered is the one resulting by the difference between the pressures and the effective areas of rebound and compression chambers (Figure 4):

$$F_{hydraulic} = F_{rebound\ chamber} - F_{compression\ chamber} \qquad (2)$$

where:

$$F_{rebound\ chamber} = \left(A_{pt} - A_{rod}\right) \bullet p_{reb} \qquad (3)$$

And:

$$F_{compression\ chamber} = A_{pt} \bullet p_{com} \qquad (4)$$

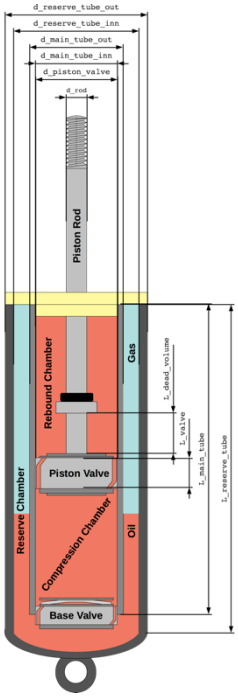

Figure 4. Damper Layout & Nomenclature

Valve Sub-Model

The flow model links the flow rates passing through the valves with the pressure drop in the chambers.

The flow passage depends on the components, which are present in the valve. The pressure drop between the chambers is related to the topology of the valve system, defined by each components properties (both rebound and compression side).
A shim valve, like the one modeled, is usually composed by a combination of:

1. Bleeding discs (Figure 5);
2. High speed discs (Figure 6);
3. Flat discs (Figure 7);
4. Check valve.

The equation used to simulate the flow rate through the valve is:

$$Q = \sqrt{\frac{2(\Delta p_{1-2} - \Delta p_0)}{\rho}} C_D A_{eff} \qquad (5)$$

which derive from the Bernoulli's equation for turbulent flow.
In the equation (5), the terms are:

1. Δp_0 preload applied to a component;
2. C_D discharge coefficient, which takes into account the ratio between the actual and the theoretical flow (similar to a mechanical efficiency);
3. A_{eff} effective Area, which is the area constricting the flow.

The effective area is the parameter that really differentiate a component with respect to another one.

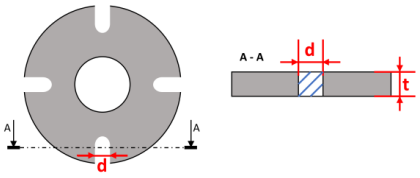

Figure 5. Bleeding Disc

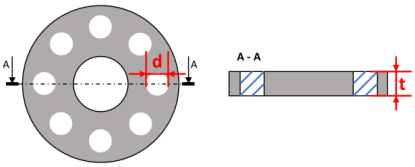

Figure 6. High Speed Disc

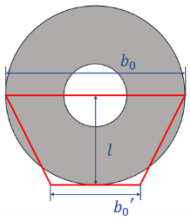

Figure 7. Flat Disc Modeling – Shim vs. Beam

Bleeding and High Speed Discs

The effective area characterizing the bleeding disc and the high speed disc is fixed and dependent on parameters like:

1. d_{hole} the diameter of the hole or the width of the apertures in the disc;
2. t_{disc} the thickness of the disc;
3. n_{holes} the number of holes (or apertures) in the disc.

The layout of the holes defines the discharge coefficient.

Flat Discs

In this case the effective area is variable, depending on the deflection of the discs. To obtain a relation between the valve pressure drop and the effective area, the deflection law of a cantilever beam has been used. The first task was to define the optimal shape of a cantilever to represents the disc shape. The best balance between "easy to use" law and "error in shape" was found by using a trapezoidal shape (Figure 7).
The deflection *f* of a trapezoidal beam subject to a load *F* with a stiffness *k* [13] is given by the equation:

$$f = \frac{F}{k} = \frac{ql}{k} \qquad (6)$$

In case of a shim stack, the force will not be a concentrated load *F* but a distributed load *q* caused by the flow acting a pressure *p* on the disc surface A_{disc}, so:

$$\begin{cases} F = \frac{1}{2} \bullet p \bullet A_{disc} \\ F = q \bullet l \end{cases} \qquad (7)$$

and:

$$q = \frac{p \bullet A_{disc}}{2l} \qquad (8)$$

It often happens that the diameter or the thickness of discs composing the shim stack are not the same. The thickness *h*, which contributes for the beam's inertia I_0, is measured as the sum of the thickness of each of the discs composing the shim stack, considering also the thickness of the bleeding discs. The overall diameter is the mean diameter of all discs. Concluding, the final equation of the effective area A_{eff} is:

$$A_{eff} = A_{eff}(f) = crf_{mean} \bullet f \qquad (9)$$

where:

$$crf_{mean} = \pi \bullet d_{mean} \qquad (10)$$

and:

$$f = \frac{F}{k} = \frac{q \bullet l}{k} = \frac{\left(\frac{p \bullet A_{mean}}{2 \bullet l}\right) \bullet \alpha \bullet l^4}{8 \bullet E \bullet I_0} \qquad (11)$$

Check Valve

The effective area characterizing the flow restricted by a check valve is proportional to the stiffness of the spring, which is pushing the valve disc against the high speed disc. The principle to model the check valve behavior is very similar to the one used for the flat discs in the shim stack, with the difference that in this case the stiffness k of the spring, which most of the time is a conical spring (Figure 8), is evaluated as the equation:

$$k_{spring} = \frac{d^4 \bullet G}{n_{active\ coil} \bullet (r_1 + r_0) \bullet (r_1^2 + r_0^2) \bullet 16} \qquad (12)$$

where G is the shear modulus, equal to:

$$G = \frac{E}{2 \bullet (1 + \nu)} \qquad (13)$$

with ν = 0.33 as Poisson's ratio for steel components.

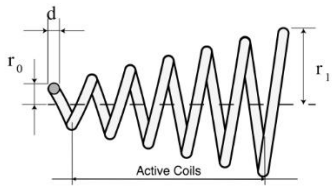

Figure 8. Conical Spring

Model of Oil Compressibility

The isothermal oil compressibility, which accounts for "the relative decrease of the volume of a system with increasing pressure in an isothermal process" [14], is the reciprocal of the oil bulk modulus.
The ADM has two different ways to account for the compressibility of the oil: one is to use a value of the compressibility constant over pressure (α_{oil}), while the other one is to use a value of the compressibility variable over pressure ($\alpha_{oil}(p)$). To define $\alpha_{oil}(p)$, different models have been analyzed and the one developed by Boes has been selected [15].
The biggest difference between the models is how they estimate the value of the bulk modulus β_{oil} at very low pressure. The equation developed by Boes (valid for low pressure systems < 100 bar) is calculating the bulk modulus as a function of pressure:

$$\beta_{oil}(p) = 0.5 \bullet \beta_{oil,ref} \bullet \log\left(99 \bullet \frac{p}{p_{ref}} + 1\right) \qquad (14)$$

where:

$$\beta_{oil}(p) = \frac{1}{\alpha_{oil}(p)} \qquad (15)$$

Friction Model

The main friction in a shock absorber is caused by steel to rubber (or elastomer) contacts, as piston tube to valve sealing and piston rod to top guide. All these pairings contribute to Coulomb and Stiction friction. The oil in the damper is also contributing to the overall friction (viscous friction).
Most mathematical formulations of friction are depending on the sign (i.e. direction) of the speed. This can lead to numerical instability, that need to be avoided because it is affecting the overall model performance. One of the most complete friction models, specifically conceived to avoid such discontinuities (Lu-Gre friction model [16, 17]).
A comparison between a simple Coulomb & Viscous friction model and the LuGre model is shown in Figure 9, where it is possible to note that the LuGre model is able to develop a continuous friction force, with a defined rise time. Figure 9b shows the hysteresis effect, not present in the simple Coulomb & Viscous friction model.
The LuGre model is an empirical dynamic friction model based on the elasticity in the contact: being empirical, a test focused on friction evaluation is needed. This is one of the reason for defining the quasi-static testing protocol described in next section.
The equations used in the LuGre friction model is:

$$F_{friction} = \sigma_0 z(t) + \sigma_1 \frac{dz(t)}{dt} + F_{viscous} v(t) \qquad (16)$$

where:

$$\frac{dz(t)}{dt} = v(t) - \frac{\sigma_0}{g(v(t))} z(t)|v(t)| \qquad (17)$$

and:

$$g(v(t)) = F_{coulomb} + (F_{stiction} - F_{coulomb}) e^{-\left|\frac{v}{v_s}\right|^{\eta}} \qquad (18)$$

The variable $z(t)$ represents the friction state and can be interpreted as the mean deflection of the junctions between two sliding surfaces.
The variable σ_0 describes the stiffness for a spring-like behavior for small displacements while σ_1 gives the micro-damping. The state variable $g(v)$ gives the modeling of the Stribeck effect [18].
The variables $F_{coulomb}$, $F_{stiction}$ and $F_{viscous}$ represent respectively the Coulomb, Stiction and Viscous friction terms. The variable v_s determines how fast is $g(v)$ in approaching $F_{coulomb}$.

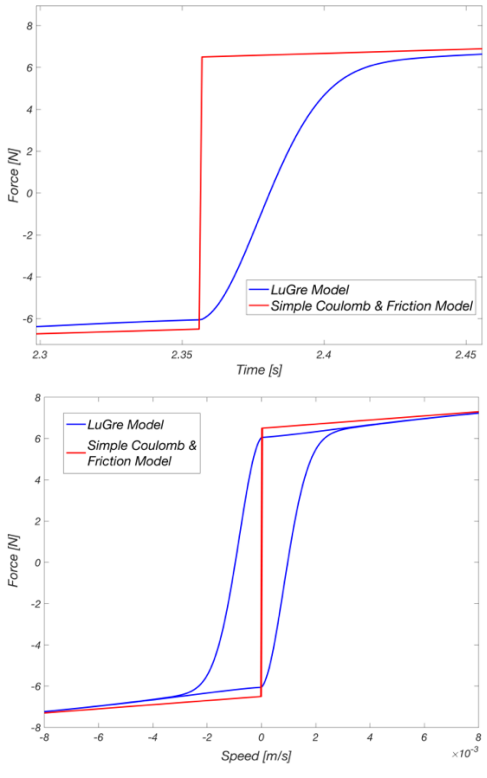

Figure 9. Coulomb vs. LuGre Friction Models Comparison: a) Time Domain and b) Speed Domain

New Testing Protocol

The protocol contains two main parts:

1. **Quasi-static** tests, performed at very low speed, with focus on friction;
2. **Dynamic** test, performed to capture the dynamic damping performance.

Each test has been thought and developed in order to capture the most of the behavior of a shock absorber and to parametrize also the CAE lump model.

Quasi-static Testing Protocol

The quasi-static testing protocol analyzes the behavior of the damper at very low speed, where most of the force is produced by the gas compression and by the friction.
The tests performed in the quasi-static testing protocol are:

1. *Travel Check* Test;
2. *GFBA* (Gas-, Friction and Break-Away Force) Test;
3. *Creep* Test;

4. *Reaction Force* Test.

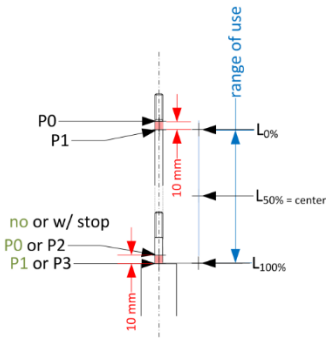

Figure 10. Range of Use

Travel Check Test

The test nomenclature is based on the points measured in this test. The travel check test is performed manually, before the operator installs the component in the testing machine. The idea is to identify the maximum available stroke of the rod and to define the so called range of use of the shock absorber (Figure 10): it is evaluated taking a 10 mm safety margin from the measure of the maximum stroke, in both rebound and compression. This safety margin is defined in order to prevent any damage to the component and to the testing machine while performing any of the tests.

GFBA (Gas-, Friction and Break Away Force) Test

The GFBA test is the most important of the quasi-static part of the protocol. It has been developed to identify the friction and the gas force of the component. It also shows the behavior of the valves in this very low speed range. It is performed using all the defined range of use stroke of the shock absorber. The component is set to Lmax and then four compressions and extensions are performed.
As can be seen in Figure 11, this test is made by a cycle of four different ramps with speeds 0.7, 1, 2 and 5 mm/s. At the end of each ramp cycle there is a holding phase of 30 seconds, to evaluate any eventual creep of the system. The test is repeated 4 times to be statistically reliable.

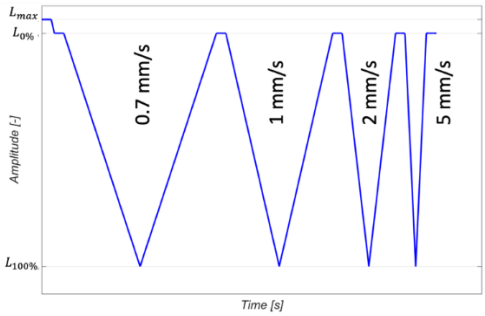

Figure 11. GFBA Test Input

Creep Test

The damper is a dynamic system, which needs time to come back to its steady-state condition once it is excited with a certain input. To evaluate this phenomenon, the creep test has been defined. The input signal of this test is made by a ramp with speed equal to 10 mm/s, starting from L_{max} position, compressing down to $L_{0\%}$, $L_{50\%}$ and $L_{100\%}$ of the component's range of use. Each compressing phase is followed by a 300 s holding phase, where the creep of the system is evaluated.

Reaction Force Test

The reaction force test is confirming the gas force value coming from the GFBA test. The principle is based on the third Newton's law (if a force is applied to the rod, the rod will rest steady until the equilibrium force is reached). When the rod begins to move, it means that a force higher than the one provided by the gas pressure has been applied. The force measured when the rod displacement is at 0.5 mm from the starting position, divided by the area of the rod, will give approximately the value of the pressure in the reserve tube.

Dynamic Testing Protocol

These new tests have been developed to improve the output coming from the standard VDA test, which is lacking in terms of:

1. resolution at low speeds in the range [0 ÷ 0.3] m/s (89% of shock absorber usage [19], where the standard VDA test has only two point ([0.055 - 0.1] m/s);
2. behavior at different amplitudes, because of the fixed amplitude (±40 mm) of the standard VDA;
3. behavior at frequency higher of 6 Hz, that is the maximum frequency achievable with above mentioned amplitude at the maximum test speed of standard VDA test (1.5 m/s).

The new tests are exploring a wider range of amplitudes, speeds and frequencies to characterize the damper performance in condition closer to the real usage. This is important to link the component performance at vehicle level, necessary to improve the overall vehicle's ride & handling behavior. Another weak point of the standard VDA test is the post-processing, which is delivering two curves. In one curve the force points are extracted at the peak of the tested speeds, in both rebound and compression (punctual analysis). In the second curve the force evolution in amplitude domain is shown ("potato diagram" - continuous analysis), to analyze the construction of the valve and if some unwanted behaviors are present (such as aeration, cavitation, stretching, etc.). The force evolution in time and speed domain is not considered, even if it is important on the damping performance evaluation. It allows to study the dynamic behavior of the shock absorber.
The introduced tests are the Advanced-VDA and the Sinusoidal Sweep. The Advanced-VDA test has been defined as an extension of the actual standard VDA test. The input, as the standard test, is characterized by a sinusoidal signal with fixed amplitude and exponentially increased excitation speed. The number of tested amplitudes has been increased from one (±40 mm) to five values (±2, 5, 10, 20, 40 mm). The ±40 mm amplitude has been maintained to have results comparable with the standard test. The same approach has been used to define the speeds at which the shock absorber will be tested. The seven speeds of the standard VDA (0.055, 0.1, 0.3, 0.6, 1, 1.2 and 1.5 m/s) have been maintained to compare the results coming from the standard VDA with the ones coming from the advanced VDA.
The Sinusoidal Sweep test has been defined as an evolution of the advanced VDA test. Instead of different speeds, the damper is excited at defined frequencies, maintaining the amplitude constant. An exponential increase of the controlled variable has been used to have a high detail at the begin of the test (low speed or low frequency). Now it is possible to analyze the damping performance in frequencies higher than 6 Hz (secondary ride). The relation between the damper behavior and the car behavior can be better understood, linking the damping performance at vehicle level. The tests are limited at 30 Hz,

considered as the border between vehicle dynamic frequencies and NVH frequencies.

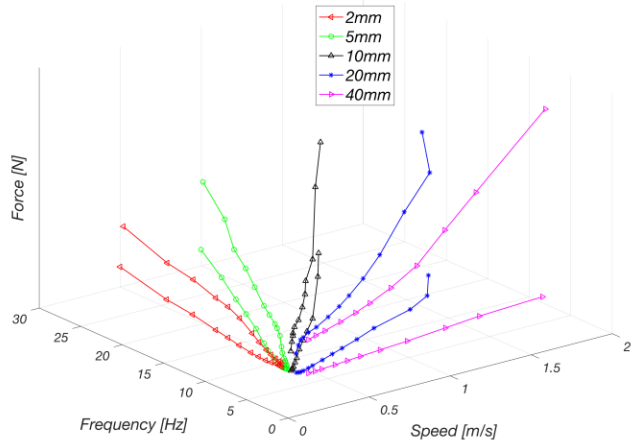

Figure 12. Example of 3D Evaluation – Force vs. Frequency vs. Speed

Post-processing and Punctual Analysis

With the punctual analysis, the damping characteristic is displayed in a three-dimensional way (Force vs. Frequency vs. Speed), as shown in Figure 12. This new way to look on the damping performance allows the component to be analyzed not only by the excitation speed, but also by the frequency of excitation, that correspond to real working condition of the damper and of the vehicle, which dynamics are normally evaluated in frequency.
Figure 13 shows the high density of measured force points in the speed range [0÷0.3] m/s. This level of detail enables better evaluation of very important features, like the rebound knee in the damper curve. All the tests are building the same curve in speed domain; this gives the proof that, looking only on speed domain, is not simple to relate the damping performance to the car behavior. On the other hand, this shows that the characteristic curve (punctual force in speed domain) can be an useful tool for tuning due to its invariant behavior over amplitude.
In figure 14, the force is plotted in the frequency domain and this is the researched link between the shock absorber and the car frequency behavior (frequency division is indicative and taken from HMG Ride & Handling Evaluation Method). It is possible to highlight the force evolution at different frequency levels and the differences between the five tested amplitudes of the test. The characteristic curve, shown in Figure 13, can be used to study:

1. The concavity and the gradient of the curve before the knee, in both rebound and compression, for body motion control and steering sensitivity.
2. The ratio between the force in rebound and in compression before the knee, important to have a solid-feel of the vehicle.
3. The knee of the curve, its position and its roundness (smooth or abrupt), relevant for comfort and noise.
4. The gradient of the curve at high speed, crucial to give mechanical stability of the vehicle on severe handling maneuver.

In the frequency curve (figure 14) is useful to study the sliding of the knee of the curve over different frequency and the linearity of the curve at high frequency. These curves are also used for the model correlation. Every change in the curve's gradient correspond to a specific component of the valve. Important examples are the knee and the subsequent linear gradient of the curve, related to the initial deflection and the stiffness of the shim stack.

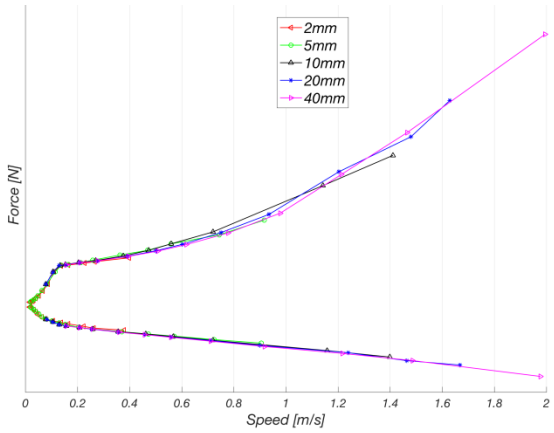

Figure 13. Force vs. Speed

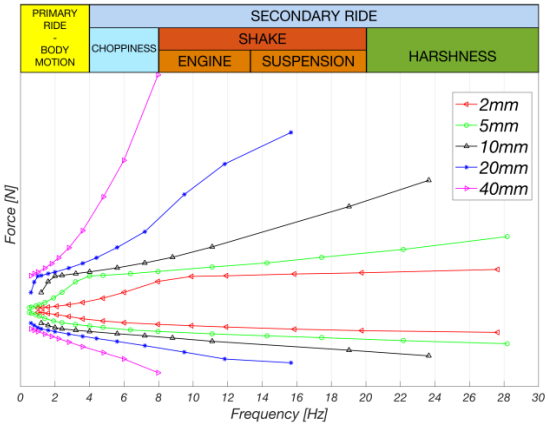

Figure 14. Force vs. Frequency

Post-processing - Continuous Analysis

With this kind of post-processing it is possible to study numerous additional characteristics of the component. In a continuous analysis phenomena related to valve and fluid design, like the hysteresis, the aeration or the cavitation, are considered. These are all fundamental aspects that need to be taken into account, directly linked to the damper construction. It is possible to obtain the force in time, amplitude and speed domain to can describe different aspects of the damping performance.

Valve Design

The shim deflection can be analyzed from both amplitude and speed domain. A change in the curve's gradient is related to a different component of the valve coming into action. This is visible especially at low frequency where the dynamic effects of the oil are still negligible. It is possible to evaluate the effective transition (smooth or abrupt) of the blowoff valve opening point. To validate the model is important to catch not only the force at a specific speed, but also the overall behavior during the transient phase.

Hysteresis

The hysteresis is more evident while increasing the excitation frequency. This aspect is not evident with a punctual analysis but it plays an important role on the damper behavior. The peak force is defined by the valve design but the transition is governed by fluid dynamic factors, such as oil inertia, oil compressibility and oil temperature. At high frequency the valve acts as a wall for the fluid, allowing no passage from a chamber to the other. This gives the round shape to the force in the speed domain.

Aeration and Cavitation

The aeration is a phenomenon present when the damper is excited at high speed and high amplitude. These circumstances lead to an increase of the fluid and gas temperature and the gas is leaked into the rebound chamber. This is stated to be the cause of compression lag, together with the cavitation phenomenon. In these highly dynamic conditions, some gas that is present in the oil at ambient pressure could also form bubbles of air into the fluid itself. This phenomenon, called cavitation, reduces the durability performance of the damper [20].

Advanced Damper Model Validation

A comparison between GFBA test and the Sinusoidal Sweep is performed (Figure 15) between the outputs coming from the ADM (displayed in red), the Dynamometer Test Bench (displayed in blue) and the 1D Lookup Table normally used in HMETC standard numerical simulation (displayed in green), filled with the 7 points coming from the standard VDA test. During the movement, the force evolution in amplitude domain rotates clockwise, while the one in speed domain rotates anticlockwise. The model correlation will be resumed in tables containing the standard deviation of the results (Std. Dev.) and the root mean square (RMS) of the residuals, in percentage with respect to the ones coming from the test bench.

GFBA Test Simulation

In Figure 15 a) is displayed that the ADM is representing, without any significant difference, the shock absorber behavior during the test. The model is slightly overestimating the force during the rest phase in $L_{0\%}$ position (see point ①). In amplitude domain (Figure 15 b)) it is possible to highlight a difference in compression. A concavity is present in the test bench curve, which is not well represented by the model, that is much more linear. This behavior could be related to the gas adiabatic law used in the model. Using the real-gas law should give better results, but with an increase of the model complexity. The improvement in terms of capability of the ADM to represent the real force evolution, with respect to the one of the one-dimensional lookup table, is quite well stated and visible. The lookup table is giving only an approximation of the mean value of the force at a determined speed. Table 1 shows the level of correlation.

Table 1. GFBA Correlation

GFBA Test	**ADM**	**1D Lookup Table**
Std. Dev. [%]	95	43
RMS Residuals [%]	98	91

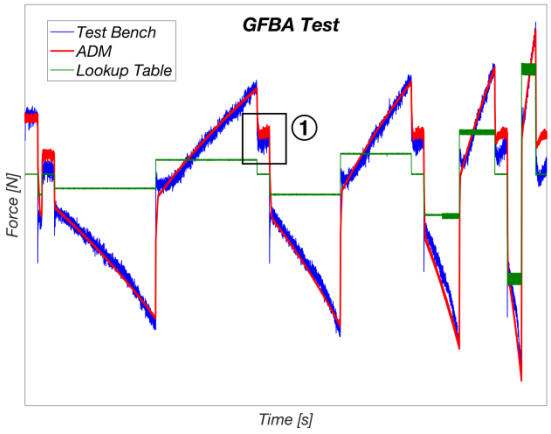

a)

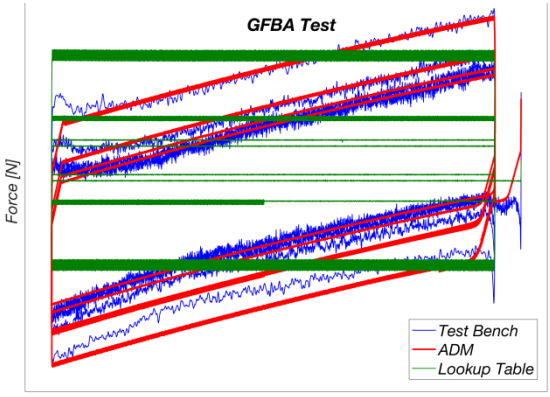

b)

Figure 15. GFBA Test Simulation results: a) Force vs. Time and b) Force vs. Amplitude

Sinusoidal Sweep Test Simulation

The validation of the model will be performed with both the continuous and the punctual analysis.

Continuous Analysis

The results at low frequency shows the hysteresis level. It is mostly determined by the valve setup and by friction and it is well represented in the ADM, while it is not represented at all in the simulations performed using the lookup table. The model is well predicting the behavior of the shock absorber in terms of absolute force value in all the domains (Figure 16). At high frequency (> 4 Hz), the model is not completely capable to estimate the overall hysteresis, but it is still able to represent the peak force (Figure 17). Tables 2 and 3 show the level of correlation at low and high frequency respectively.

Table 2. Low Frequency Sinusoidal Sweep Correlation

Low Freq. Sweep Test	**ADM**	**1D Lookup Table**
Std. Dev. [%]	96	88
RMS Residuals [%]	71	61

Table 3. High Frequency Sinusoidal Sweep Correlation

High Freq. Sweep Test	**ADM**	**1D Lookup Table**
Std. Dev. [%]	95	89
RMS Residuals [%]	56	17

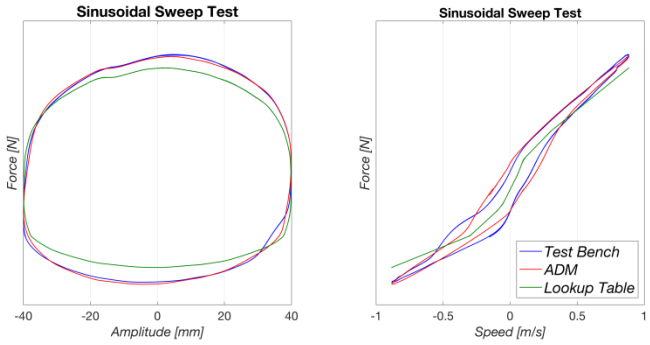

Figure 16. Low Frequency Correlation: Amplitude 40 mm and Frequency 3.5 Hz

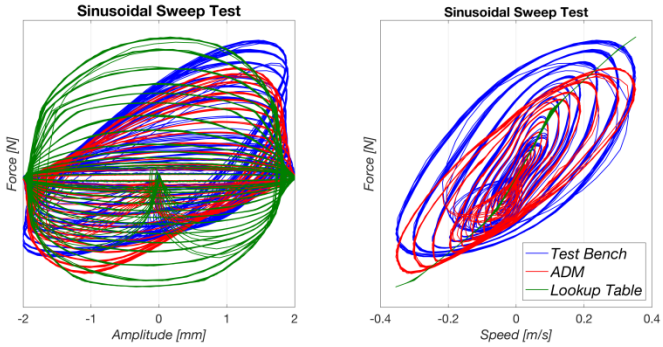

Figure 17. High Frequency Correlation: Amplitude 2 mm and Frequency 0.5 ÷ 3 Hz

Punctual Analysis

Analyzing only the force punctual values, how it is developed by the damper is not taken into account. This is a good and easy representation of the shock absorber characteristic, especially in speed and frequency domains. The level of correlation is shown in Table 4.

Table 4. Sinusoidal Sweep - Punctual Correlation

Sinusoidal Sweep Test	**ADM**	**1D Lookup Table**
Rebound [%]	96	82
Compression [%]	98	83

Main Results

Improved Damper Performance

The new testing protocol enables HMETC to have a higher amount of information about the damper performance has been developed.

First of all it gives high detail in speed domain (Figure 18), especially on the low-speed range, fundamental area to ensure body control and comfort.

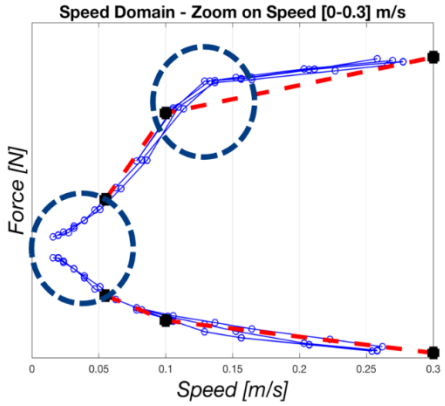

Figure 18. Speed Domain, Standard VDA (red) vs. Advanced VDA (blue)

Second, the shock absorber can be studied in frequency domain. In this way a better connection between component and vehicle performance is established (Figure 19).

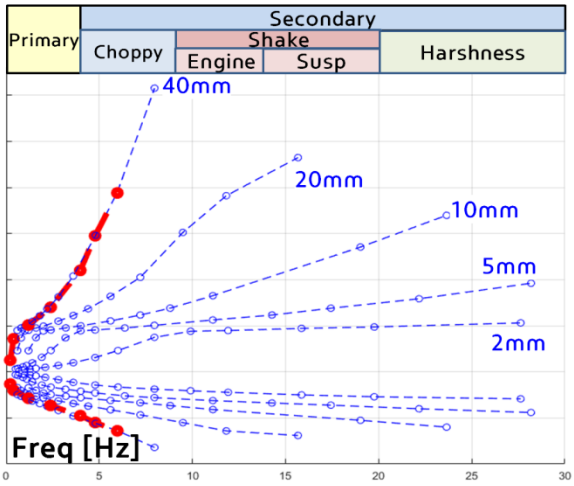

Figure 19. Frequency Domain, Standard VDA (red) vs. Advanced VDA (blue)

ADM – Tuning Sensitivity

To show the potentiality of this new tool, a sensitivity study has been performed and the sinusoidal sweep test has been simulated. In a first loop, the number of holes in the bleeding disc (Figure 20) have been changed (±50%), while in a second loop the thickness (±50%) of the flat discs (figure 21). Both the changes have been made on the rebound side of the valve. As damper tuning is one of the most time-consuming activity during the vehicle development process, this new tool can guide the tuner in solving how to obtain the wanted damper behavior. Additionally the model can be used in a total virtual vehicle environment (CAE) or at the driving simulator (during redevelopment phase) as a tool for virtual tuning. This tool gives the possibility to represent the real construction of the damper and reducing the spread between virtual and real world.

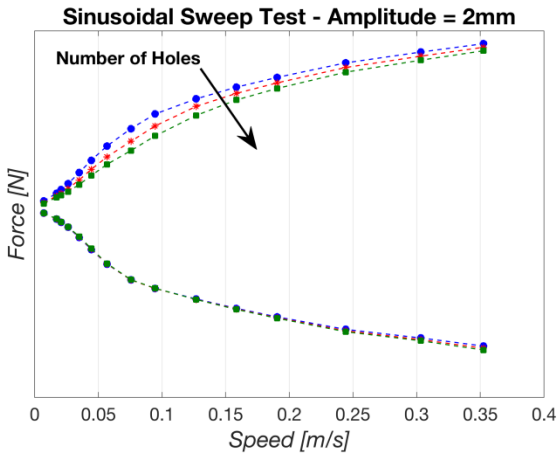

Figure 20. Model Sensitivity, Holes Number in Bleeding Disc

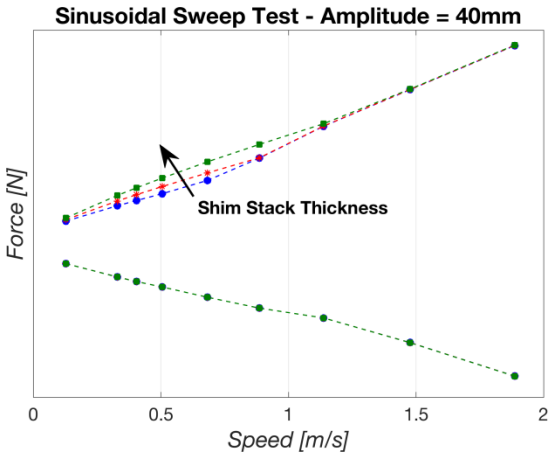

Figure 21. Model Sensitivity, Shim Stack Stiffness

Conclusions

A higher understanding of the damper performance connected to the overall vehicle performance is ensured by the new testing protocol and by the ADM. The new testing protocol is offering the frequency analysis of the damper together with a higher detail in speed domain. The Advanced Damper Model is representing the physical component and it allows predicting even the high frequency behavior of the damper (important for ride simulation).
Today damper tuning is a highly time-consuming activity, mainly linked to subjective feeling of tuner's experience.
The New Testing Protocol, with the link from component to vehicle performance, and the Advanced Damper Model, permitting the so-called Virtual Damper Tuning, will enable HMG to reduce the development time and costs, increasing at the same time the quality of the products. This is fundamental from an OEM point of view.
In the next future HMETC will continue to improve the testing protocol, focusing on testing time reduction and frequency-dependent behavior of the damper, and the advanced damper model, focusing on different valves modeling and real-time applications.

References

1. Carello M., Brusaglino G., Razzetti M., Carlucci A.P., Doria A., Onder C.H., "New technologies demonstrated at the Formula Electric and Hybrid Italy 2008", 24th International Battery, Hybrid and Fuel Cell Electric Vehicle Symposium and Exhibition EVS24, Stavanger (Norway) 13-16 May 2009, World Electric Vehicle Journal, Vol. 3, Issue 1, 2009, ISSN: 20326653.
2. Filippo N.; Carello M.; D'Auria M.; Marcello A., "Optimization of IDRApegasus: Fuel Cell Hydrogen Vehicle" SAE International Congress, Michigan (USA) 16-18 April, pp. 9, 2013, DOI: 10.4271/2013-010964.
3. Ferraris, A.; Xu, S.; Airale, A.G.; Carello, M., "Design and optimization of XAM 2.0 plug-in powertrain", International Journal of Vehicle Performance, Inderscience, pp. 25, Vol. 3, 2017, ISSN: 1745-3208, DOI: 10.1504/IJVP.2017.10004910.
4. Carello, M., De Vita, A., Ferraris, A., "Method for Increasing the Humidity in Polymer Electrolyte Membrane Fuel Cell", Fuel Cells, Vol. 16, Issue 2, pp. 157-164, April 2016, ISSN: 1615-6854, DOI: 0.1002/fuce.201500110.
5. De Vita A., Maheshwari A., Destro M., Santarelli M., Carello M., "Transient thermal analysis of a lithium-ion battery pack comparing different cooling solutions for automotive applications", Applied Energy, pp. 12, 2017, Vol. 206, ISSN: 0306-2619, DOI: 10.1016/j.apenergy.2017.08.184
6. Cubito C.,, Rolando L., Ferraris A., Carello M., Millo F., "Design of the control strategy for a range extended hybrid vehicle by means of dynamic programming optimization", IEEE Intelligent Vehicles Symposium (IV), Los Angeles, CA, USA 11-14 June 2017, pp. 8, 2017, Vol. 1, ISBN: 978-1-5090-4804-5, DOI: 10.1109/IVS.2017.7995881
7. Cittanti D., Ferraris A., Airale, A.G., Fiorot, S., Scavuzzo S., Carello, M. "Modeling Li-ion batteries for automotive application: A trade-off between accuracy and complexity", International Conference of Electrical and Electronic Technologies for Automotive, Torino 15-16 June 2017, pp. 8, 2017, ISBN: 978-88-87237-26-9, DOI: 10.23919/EETA.2017.7993213.
8. Genta, G., Morello, L., "The automotive chassis", Vol. 1-2, Springer, 2009.
9. Gillespie T.D., "Vehicle dynamics", Warren date, 1997.
10. Guiggiani M., "The science of vehicle dynamics: handling, braking ride of road and race cars", Springer Science, 2014.
11. Duym S.W., "Simulation tools, modelling and identification for an automotive shock absorber in the context of vehicle dynamics", Vehicle System Dynamics, 33 (4), pp.261-285, 2000.
12. Duym S., Stiens R., Baron V., Reybrouck K.G., " Physical modelling of the hysteretic behavior of automotive shock absorbers", SAE Technical paper, 1997.
13. Bongiovanni G., Roccati G., "Le molle: tipi e criteri di calcolo", Levrotto & Bella, Italy, 1994.
14. American Meteorological Society, "Glossary of Meterorology – Coefficient of Compressibility", 2012.
15. Boes C., "Hydraulische Achsantiebe im digitalen Regelkreis", 1995.
16. De Wit, C.C, Olsson H., Astrom K.J., Lischinsky P., "A new model for control of systems with friction", IEEE Transaction on automatic control, 40 (3), pp. 419-425, 1995.
17. Do N.B., Ferri A.A., BAuchau O.A., "Efficient simulation of a dynamic system with lugre friction", Journal of Computational and Nonlinear Dynamics, 2(4), pp. 281-289, 2007.
18. Armstrong-Hélouvry B., Dupont P., De Wit C., "A survey of models, analysis tools and compensation methods for the control of machines with friction", Automatica 30 (7), pp. 1083-1138, 1994.
19. Fukushima N., Hidaka K., Iwata K., "Optimum characteristics of automotive shock absorbers under various driving conditions

and road surfaces", International Journal of Vehicle Design, 4 (5), pp. 463-472, 1983.
20. Dixon J.C., "The shock absorber handbook", John Wiley & Sons, 2008.

Contact Information

Alessandro Salgarello
asalgarello@hyundai-europe.com

Daniel Hahn
dhahn@hyundai-europe.com

Antonino Pizzuto
apizzuto@hyundai-europe.com

Massimiliana Carello
Politecnico di Torino – Department of Mechanical and Aerospace Engineering
C.so Duca degli Abruzzi, 24 -10129 Torino – Italy
Phone: +39.011.0906946
massimiliana.carello@polito.it

Alessandro Ferraris
alessandro.ferraris@polito.it

Andrea Giancarlo Airale
andrea.airale@polito.it

Acknowledgments

Thanks to the complete Chassis Team in Engineering Design of Hyundai Motor Europe Technical Center that supported this activity, from technical and human point of view. Hyundai Motor Europe Technical Center is the European R&D technical center for Hyundai Motor Group (more information are available at www.hmetc.com).

Definitions/Abbreviations

OEM Original Equipment Manufacturer
R&D Research & Development
CAE Computer Aided Engineering
VDA Verband der Automobilindustrie (German Association of the Automotive Industrie)
Crf Circumference [m]
Area [m^2]
E Young Modulus [Pa]
β Bulk Modulus [Pa]
G Shear Modulus [Pa]
l Length of Cantilever Beam [m]
q Distributed Load [N/m]
F Force [N]
Pt Pressure tube
R Radius [m]
P Density [kg/m^3]
P Pressure [Pa]
K Stiffness [N/m]
D Diameter [m]
I_0 Cantilever Beam Moment of Inertia [m^4]
R Radius [m]
ν Poisson's Coefficient [-]